THE ASTROPHYSICAL JOURNAL, 287:952–958, 1984 December 15

APPARENT SOLAR TEMPERATURE ENHANCEMENT DUE TO LARGE-AMPLITUDE WAVES

W. KALKOFEN
Harvard-Smithsonian Center for Astrophysics
AND
P. ULMSCHNEIDER AND F. SCHMITZ
Institut für Theoretische Astrophysik, Heidelberg
Received 1983 February 28; accepted 1984 June 11

ABSTRACT

We suggest that the discrepancies in the temperature structure between recent empirical solar model atmospheres that are based on observations of the infrared continuum or the ultraviolet resonance lines of Ca II and Mg II are caused, at least in part, by acoustic-type slow-mode magnetohydrodynamic waves.

In a time-dependent model atmosphere in which acoustic waves travel outward, the amplitude becomes large in the temperature-minimum region between photosphere and chromosphere. Because of the nonlinear response of the Planck function to temperature fluctuations, the temperature peaks are weighted preferentially in the ultraviolet lines. Hence the time-averaged radiative fluxes in the Ca and Mg lines are enhanced relative to the flux in the infrared continuum. When the emergent radiation from the time-dependent model is analyzed with the aid of static models, the increased fluxes in the ultraviolet lines relative to the flux in the infrared continuum lead to inferred temperatures that depend systematically on the spectral features used in the analysis. These enhanced temperatures are in qualitative agreement with the discrepant values for the minimum temperature in existing empirical solar models.

Numerical calculations for (horizontally) uniform heating with a mechanical energy flux consistent with the observed cooling rate of the solar chromosphere give enhancements for the minimum temperature between the photosphere and the chromosphere that are smaller than those of the empirical models. The observed enhancements can be reproduced if the mechanical flux is increased—which implies a reduction in the surface area heated *directly* by waves. This may suggest that mechanical heating takes place not uniformly over the solar surface but in smaller regions, perhaps in magnetic flux tubes.

Subject headings: radiative transfer — Sun: atmosphere — Sun: chromosphere

I. INTRODUCTION

Empirical models of the solar photosphere and chromosphere are based either on continuum or on line observations. Continuum models (Gingerich *et al.* 1971; Vernazza, Avrett, and Loeser 1973, 1976, 1981) use a broad range of continuum intensity observations in the visible, ultraviolet, and infrared spectral ranges. Line models (Ayres and Linsky 1976; Linsky and Ayres 1978) exploit mainly the intensity observations of the strong resonance lines of Ca II and Mg II. As discussed by Avrett (1977), there are considerable differences not only between continuum and line models but also between line models based on different lines. Near the temperature minimum, for example, the Ca II line models are approximately 300 K hotter than the continuum models, and the Mg II line models are 100–200 K hotter than the Ca models (Ayres and Linsky 1976, Fig. 7; Linsky and Ayres 1978, Fig. 1). These differences cannot be attributed to the data reduction alone. Indeed, the discrepancy between the empirical solar Ca II and Mg II line models, which are determined in a very similar fashion, suggests that a physical effect is involved. To identify this effect is important not only for the solar atmosphere but also for the atmospheres of other late-type stars because the present empirical models for nonsolar chromospheres are based entirely on lines (cf. Linsky 1980).

One reason for the discrepancies between models may be the assumption of a one-dimensional, horizontally homogeneous atmosphere made for both line and continuum models. Basri and Linsky (1979), for example, note that the emission in the near-UV resonance lines is weighted preferentially by the hotter components of the atmosphere, while the visible continuum emission is more evenly weighted by the thermal irregularities. A static two-component model described by Ayres (1981), where the ultraviolet resonance line emission arises mainly in hot flux tubes that penetrate a cooler photosphere dominated by CO emission, attempts to account for the difference between the various empirical models. However, because of efficient radiation damping it is difficult to support permanent structures of significantly higher temperature in the photosphere. Such structures could be maintained only by large amounts of mechanical heating. But the possibilities for heating thin flux tubes efficiently at heights considerably below the temperature minimum are limited. The only likely mechanism is shock dissipation of acoustic-type slow-mode magnetohydrodynamic (mhd) waves. For shocks to form at photospheric heights, the waves must have high amplitude and a very short period. However, such waves suffer very strong radiation damping in the photosphere (cf. Ulmschneider and Kalkofen 1977), and it is very unlikely that such damping would allow shocks to form, since the wave amplitude would tend to remain low and in the linear regime.

Another explanation for the discrepancies between the empirical solar models might be the dynamical nature of the atmosphere. In the construction of the (semi)empirical models, hydrostatic equilibrium is assumed and time-

dependent phenomena are neglected. Kalkofen (1979, private communication reported in Ulmschneider 1979) has suggested that part of the discrepancy between the models might be due to time-dependent phenomena such as acoustic waves, in which the nonlinearity of the Planck function with respect to temperature leads to preferential weighting of the temperature peaks of large-amplitude waves, thus giving rise to the apparently high temperatures observed in the ultraviolet part of the spectrum (cf. Kalkofen 1981).

For purely acoustic heating with waves emerging (horizontally) uniformly over the solar surface and with sufficient energy flux to balance the radiative cooling rate of the chromosphere, Ulmschneider *et al.* (1978, hereafter Paper I) have shown that the temperature amplitude at the temperature minimum reaches 500 K and the velocity amplitude reaches 1 km s^{-1}, growing to 1000 K and 2 km s^{-1} in the chromosphere. This amounts to a perturbation of the thermodynamic variables of the gas at the temperature minimum by more than 10%. If, as proposed by Ulmschneider and Stein (1982) and suggested by the observations, the heating is concentrated in magnetic flux tubes—in this case the waves would be acoustic-type slow-mode mhd waves—the amplitudes may be even larger.

Large wave amplitudes will have a considerable influence on the integrated Planck function, which depends on temperature as T^4. The effect will be even larger in the ultraviolet, where the monochromatic Planck function of the K line of Ca II at the temperature minimum depends on T as T^8 and that of the k line of Mg II, as T^{12}. Because of this strong temperature dependence, the excess of emission from the high-temperature part of a large-amplitude wave will not be balanced by the deficit of emission from the low-temperature part. Thus, temperature fluctuations will make the Ca line appear brighter than the frequency-integrated continuum, and the Mg line, in turn, brighter than the Ca line.

The time scale of the hydrodynamic phenomena described above might be of the order of a minute or less. But the observations typically average over a much longer time interval. Therefore, only the time average of the monochromatic flux is observed. The observations are then interpreted by means of time-independent models. In these empirical models, the higher time-averaged flux of the dynamical atmosphere results in higher apparent temperatures. Thus the empirical models, because they are static, should lead to inferred temperatures that increase systematically with the frequency of the observed spectral feature. This is indeed the sense of the difference between empirical models based on the infrared continuum and on the Ca and Mg lines. Qualitatively, the dynamical model can therefore explain the discrepancy between the empirical models of the solar atmosphere as well as the "temperature enhancement" of empirical stellar photospheres (cf. Linsky 1980; Kelch 1978; Kelch *et al.* 1978; Kelch, Linsky, and Worden 1979).

In order to lend further support to the proposition that the different values of the minimum temperature in empirical solar models are caused by the nonlinear response of the Planck function to mhd waves of large amplitude, we compute the magnitude of the effect. However, calculations of magnetic tube waves consistent with the heating requirements of the chromosphere have not been performed. The wave amplitudes are therefore uncertain. But the spatially homogeneous acoustic wave calculations of Paper I should be adequate to estimate the amplitudes involved, and detailed radiative transfer calculations should at least indicate the magnitude of the effect as far as the discrepancy of the Ca II and Mg II line models at the temperature minimum is concerned.

We note that in related work, Gouttebroze and Leibacher (1980) have investigated the effect of chromospheric oscillations with periods near 3 and 5 min on the same resonance lines. Their aim was to study the asymmetry and the Doppler shifts of the emergent line profile; their attention was focused on the emission and central absorption features and therefore on the time-dependent behavior of layers higher in the chromosphere.

Section II describes the radiative transfer method, § III discusses the numerical results, and § IV draws pertinent conclusions.

II. THE TRANSFER CALCULATION

a) The Model Atmosphere

The temperature distributions for an acoustic wave propagating in the solar atmosphere are shown in Figure 1; also indicated are the initial radiative equilibrium and time-averaged temperature distributions, T_{RE} and $\bar{T}$. The details of the hydrodynamic calculation are described in Paper I. The wave has a period of 30 s and an initial energy flux at the base of the photosphere of $F_M = 5.0 \times 10^7$ ergs cm^{-2} s^{-1}. The parameters have been chosen to be such that the wave forms a shock at the location of the observed temperature minimum and that the dissipated energy is sufficient to balance the chromospheric cooling rate. These requirements are for the idealized model without magnetic fields; these fields make the solar atmosphere horizontally inhomogeneous and concentrate the acoustic energy in magnetic flux tubes.

Figure 1 shows, from the bottom up, a time sequence covering one wave period. Every other time step of the calculation is displayed. Sufficient time has elapsed since the wave dis-

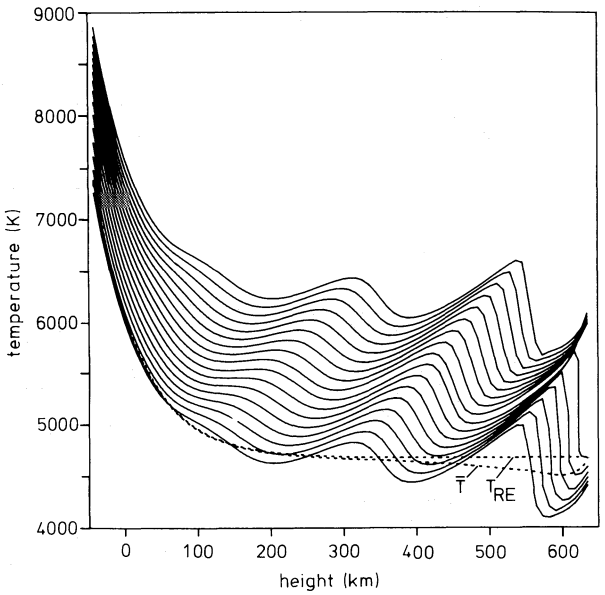

FIG. 1.—Time sequence of photospheric temperature distributions for a propagating acoustic wave with flux $F_M = 5.0 \times 10^7$ ergs cm^{-2} s^{-1} and period $P = 30$ s (drawn). The time step is 1.92 s. Time steps are separated by shifts of 100 K. The initial, radiative equilibrium and the time-averaged temperature distributions, marked T_{RE} and $\bar{T}$, are shown by dashed curves.

turbance moved into the initial radiative equilibrium atmosphere for the mean atmosphere to have reached a steady state.

b) The Model Atom and the Transfer Equation

For the calculation of the apparent temperature enhancement arising from large-amplitude acoustic waves and the nonlinearity of the Planck function it is sufficient to use an idealized version of the resonance lines of the Mg II and Ca II ions. We represent the h and k and the H and K resonance doublets by single representative lines for which the radiative transfer is computed assuming that the ions are described by two bound levels with a background continuum. The line parameters are those of the k and K lines, respectively, and are summarized in Table 1.

The oscillator strengths and the radiation damping widths, $\Gamma_{\rm rad} = A_{UL}$, are from Wiese, Smith, and Miles (1969), the abundances, $A_{\rm el}$, from Vernazza, Avrett, and Loeser (1981), and the elastic (van der Waals) collision widths, Γ_E, from Ayres (1975), with

$$\Gamma_E = \Gamma_{\rm vdW}\left(\frac{T}{5000}\right)^{0.3} n_{\rm H}\,, \tag{1}$$

where T is the kinetic temperature and $n_{\rm H}$ is the number density of neutral hydrogen. For the downward bound-bound collisional coefficient, C_{UL}, we take the value given by Shine (1973) with $C_{UL} = C_E n_e$, where n_e is the number density of electrons. We assume that both calcium and magnesium are entirely in the singly ionized state and that the electron density is given by $n_e = 10^{-4}\, n_{\rm H}$ and the hydrogen density by $n_{\rm H} = \rho/1.4m_{\rm H}$, where ρ is the mass density of the gas and $m_{\rm H}$ is the mass of a hydrogen atom.

The line transfer equation is written for a two-level atom with a background continuum (cf. Mihalas 1978, p. 350),

$$\mu\frac{dI_{\nu\mu}}{dz} = -(\kappa^C + \kappa_0^L\phi_\nu)I_{\nu\mu} + \frac{1}{2}\kappa_0^L(1-\epsilon)\int_0^\infty d\nu'\int_{-1}^{1} d\mu' R(\nu,\nu')I_{\nu'\mu'} + (\kappa^C + \kappa_0^L\phi_\nu\epsilon)B\,, \tag{2}$$

where B is the Planck function and ϵ the collision parameter,

$$\epsilon = \frac{\epsilon'}{1+\epsilon'}\,, \tag{3}$$

with

$$\epsilon' = \frac{C_{UL}}{A_{UL}}\left[1 - \exp\left(-\frac{h\nu_{UL}}{kT}\right)\right]. \tag{4}$$

The continuum absorption coefficient κ^C has been computed with the help of the ATLAS6 code of Kurucz (1979). The line absorption coefficient is

$$\kappa_0^L = n_{\rm el}\,B_{LU}\,\frac{h\nu_{UL}}{4\pi}\,\frac{1}{\pi^{1/2}\Delta\nu_{\rm D}}\,, \tag{5}$$

where

$$\Delta\nu_{\rm D} = \frac{\nu_{UL}}{c}\left(\frac{2kT}{m_{\rm el}}\right)^{1/2} \tag{6}$$

is the Doppler width; $n_{\rm el}$ is the number density of the element and $m_{\rm el}$ its mass; and the other quantities have their usual meanings. The absorption profile is given by the Voigt function (for the numerical evaluation, see Hui, Armstrong, and Wray 1978), $\phi_\nu = H(a, \nu)$, where $\nu = \Delta\nu/\Delta\nu_{\rm D}$ and $a = \Gamma/4\pi\Delta\nu_{\rm D}$, with $\Gamma = \Gamma_{\rm rad} + \Gamma_E$.

The maximum photospheric velocity amplitude (of about 5×10^4 cm s^{-1}) resulted in a frequency shift of less than 7×10^{-3} Å, which is less than a thermal Doppler width and hence of no importance for the inner wings of the lines. We therefore neglected the angle dependence of the absorption profile resulting from the Doppler shifts due to the wave motion. Thus the computed lines are symmetric. We also neglected microturbulent broadening on the assumption that the atmospheric velocity field is completely resolved. Since our interest is in the line wings down to the K1 and $k1$ minima, the influence of microturbulence on these features would be negligible even if the assumption should be invalid and microturbulence should be important.

In the line wings, partial frequency redistribution is important, but the angle dependence of the scattering process is not. Accordingly, we use the angle-averaged frequency redistribution function (Ayres 1975),

$$R(\nu,\nu') = \left[\frac{\Gamma_E}{\Gamma_{\rm rad}+\Gamma_E}\,\phi_\nu\phi_{\nu'} + \frac{\Gamma_{\rm rad}}{\Gamma_{\rm rad}+\Gamma_E}\,\phi_\nu\,\delta(\nu-\nu')\right], \tag{7}$$

and solve the transfer equation in the two-stream approximation, using the method of Grant, Hunt, and Peraiah (Grant and Peraiah 1972; Peraiah and Grant 1973; Peraiah 1978), with 37 depth and 21 frequency points.

The depth range that is important for the emergent radiation field in the line wings includes the photosphere up to the temperature minimum region but excludes the higher chromospheric layers, where the emission and central absorption features are formed. The profiles shown in Figures 2 and 3 include these central features; they are not entirely consistent with the wave model, however.

TABLE 1

LINE PARAMETERS FOR REPRESENTATIVE Mg II AND Ca II LINES

Parameter	Mg II	Ca II
λ_{UL} (Å)	2796	3933
$A_{\rm el}$	3.9×10^{-5}	2.82×10^{-6}
$\Gamma_{\rm rad}$ (s^{-1})	2.7×10^{8}	1.5×10^{8}
$\Gamma_{\rm vdW}$ (s^{-1} cm^3)	1.0×10^{-8}	1.1×10^{-8}
C_E (s^{-1} cm^3)	3.63×10^{-7}	2.92×10^{-7}

III. NUMERICAL RESULTS

a) Wing Intensities

We have compared the computed specific intensities with the partial redistribution calculations of the calcium K line by Shine, Milkey, and Mihalas (1975, Figs. 3, 4) and of the magnesium k line by Ayres and Linsky (1976), which are based on the Harvard-Smithsonian Reference Atmosphere (Gingerich *et al.* 1971, hereafter HSRA) and Vernazza, Avrett, and Loeser (1976, hereafter VAL) models. Although there is good agreement, the wings in our calculation are much flatter. This is caused by our atmospheric model, which was obtained from a time-dependent hydrodynamic calculation with gray radiative

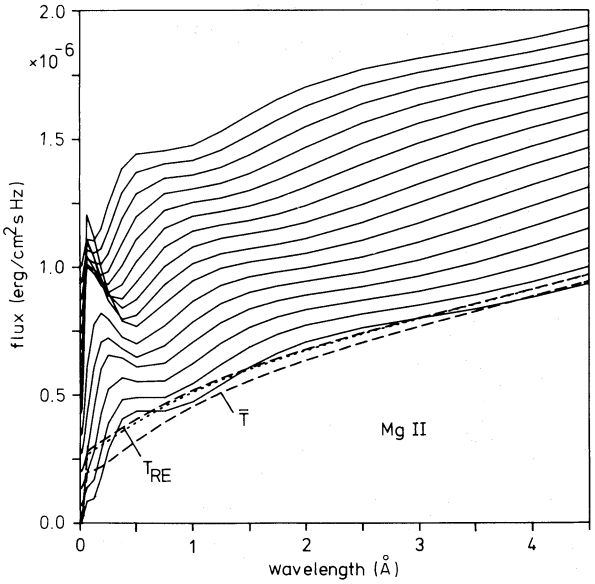

FIG. 2.—Time sequence of monochromatic fluxes, πF_ν, in a wing of the Mg II k line for the acoustic wave shown in Fig. 1. Phases are shifted by $\Delta\pi F_\nu = 6.67 \times 10^{-8}$ ergs cm^{-2} Hz^{-1}. The fluxes for the radiative equilibrium atmosphere and for the time-averaged temperature distribution are shown by dashed curves; the time-averaged flux is shown by dotted curves,

transfer. A comparison of our radiative equilibrium and time-averaged temperature distributions with the HSRA and VAL models is given in Paper I, Figure 6. The high boundary temperature of 4700 K and the low gradient of the initial gray temperature distribution readily explain the behavior of the intensity profiles. Since we are interested only in a differential effect, the model should be adequate.

b) Line Profiles

For the propagating acoustic wave of Figure 1, Figures 2 and 3 show the time sequence of the monochromatic flux in the wings of the Mg II k line and of the Ca II K line. Note that the

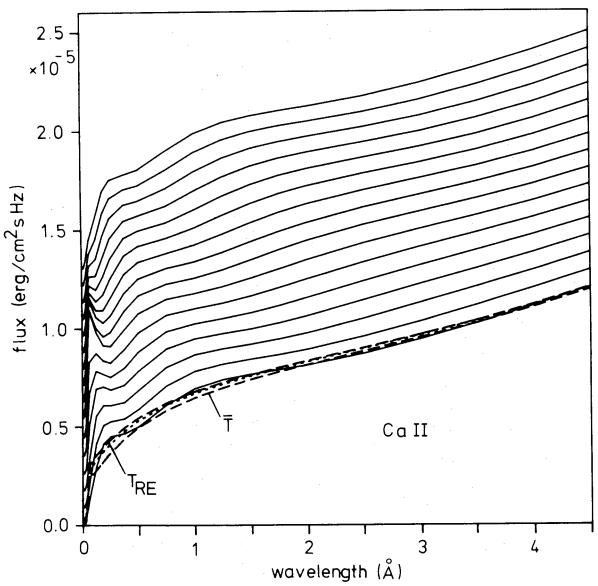

FIG. 3.—The same as Fig. 2, but for the Ca II K line, with a vertical shift of $\Delta\pi F_\nu = 8.67 \times 10^{-7}$ ergs cm^{-2} Hz^{-1}.

higher opacity in the Mg line expands the wavelength scale for the profile by a factor of about 2 relative to the Ca line. The general behavior of the profiles agrees well with the results of Shine, Milkey, and Mihalas (1975). The comparison of the temperature distributions with the flux curves indicates the source of the monochromatic flux. The upward propagation of the acoustic wave in Figure 1 appears as an inward propagation toward line center in the flux curves. The temperature maxima at 320 and 540 km of the bottom curve in Figure 1, for example, produce the relative flux maxima in the Mg line profile of Figure 2 at 2 and 0.5 Å; the temperature minima at 200 and 400 km produce the relative flux minima at 4 and 1 Å; in the Ca line (Fig. 3), the same temperature maxima and minima produce the flux maxima at 1.2 and 0.25 Å and minima at 2.5 and 0.5 Å.

Figures 2 and 3 also show that the monochromatic fluxes in the Ca and Mg lines for the initial radiative equilibrium atmosphere, marked T_{RE}, are everywhere brighter than those for the mean atmosphere corresponding to a very large number of wave trains, marked $\bar{T}$. This happens because the temperature in radiative equilibrium is everywhere higher than the temperature of the mean atmosphere after the atmosphere has reached a stastically steady state. Note, however, that the time-averaged monochromatic flux profiles (*dotted curves*) exceed the $\bar{T}$ flux profiles everywhere by a considerable amount. This behavior of the flux profiles is a consequence of the nonlinear response of the Planck function in the ultraviolet to mechanical waves of large amplitude, which makes the time-averaged line profiles differ from the profiles for the time-averaged temperature distribution. It is present even when the mean atmosphere is nearly the same as the initial atmosphere—because only very few wave trains have traversed the atmosphere—and in practically the same amount (see below).

c) Temperature Enhancements

The empirical models based on lines are time-independent. Therefore, the increased, time-averaged monochromatic flux is interpreted as implying an increased temperature. In order to estimate this temperature enhancement we have solved the line transfer equation for Ca II and Mg II in static atmospheres with temperature distributions $T(z) = \bar{T}(z) + \Delta T(z)$ such that the line profiles matched the time-averaged profiles of the dynamical atmosphere. Since the pressure distributions in the radiative equilibrium atmosphere (with T_{RE}) and in the time-averaged atmosphere (with $\bar{T}$) were nearly the same, we left the pressure distribution of the temperature-enhanced atmosphere (with $\bar{T} + \Delta T$) unchanged.

Figure 4 shows the resulting temperature enhancements, $\Delta T(z)$, for the two lines as functions of height. It is seen that the apparent temperature enhancement inferred from the Mg line is everywhere larger than that inferred from the Ca line. This is due to the stronger temperature dependence of the monochromatic Planck function at the Mg line, for which the apparent temperature enhancement relative to the time-averaged atmosphere reaches about 80 K at the temperature minimum; in the Ca line the atmosphere appears about 15 K cooler.

d) Waves with Higher Energy Flux

The temperature enhancements are due to nonlinear effects and, thus, are critically dependent on the amplitude of the assumed waves. The energy flux F_M at the top of the convection zone and the period P of the acoustic wave in Figure 1 ($F_M = 5.0 \times 10^7$ ergs cm^{-2} s^{-1} and $P = 30$ s, hereafter called

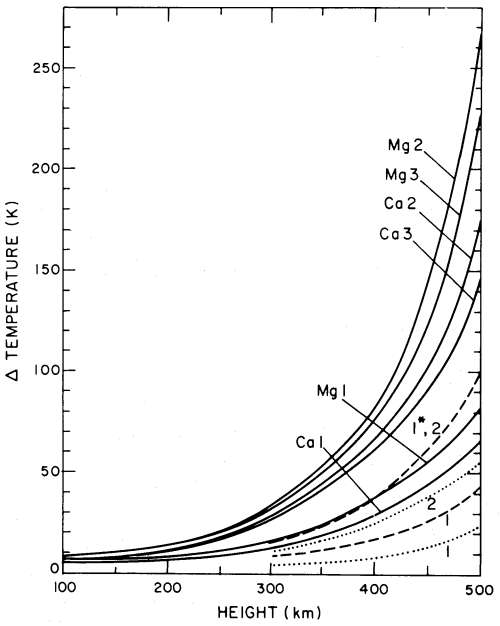

FIG. 4.—Apparent temperature enhancements (drawn) relative to the time-averaged temperature as functions of height above optical depth $\tau_{0.5\,\mu m} = 1$. The results for the Mg II and Ca II lines are shown for several acoustic wave solutions. Case 1: $F_M = 5.0 \times 10^7$ ergs cm^{-2} s^{-1} and $P = 30$ s. Case 2: $F_M = 1.0 \times 10^8$ ergs cm^{-2} s^{-1} and $P = 30$ s. Case 3: $F_M = 5.0 \times 10^7$ ergs cm^{-2} s^{-1} and $P = 60$ s. Temperature depressions (relative to the initial temperature) are shown by dashed and dotted curves. Dashed curves are for cases where the atmosphere has attained a dynamically steady state, dotted curves for cases where this state has not yet been reached. The curve labeled *1** shows the temperature depression for the approximate opacity formula described in the text; the other temperature depression curves are for calculations with the Kurucz opacity table.

case 1) were chosen to satisfy three conditions: the observed height of the temperature minimum as well as the empirical chromospheric radiation loss must be reproduced approximately, and the energy flux must emerge homogeneously distributed over the solar surface. The last assumption is unrealistic, since the Ca II and Mg II line emission occurs preferentially in regions of high magnetic field strength. If, as assumed by Ulmschneider and Stein (1982), the waves that balance the empirical radiation loss are restricted to a small part of the solar surface, they must carry more energy flux. From the models of Vernazza, Avrett, and Loeser (1981) and of Avrett (1981) one can deduce, for example, that the chromospheric radiation loss from the bright network (their model F) is larger by a factor of 2.3 than the chromospheric radiation loss from the average quiet chromosphere (their model C) (cf. also Withbroe and Noyes 1977). Now larger energy fluxes require larger wave amplitudes. Since detailed mhd calculations for tube waves have not yet been performed, we illustrate the effect of such waves with two calculations for acoustic waves computed in Paper I. In the first case (hereafter called case 2), the energy flux is doubled ($F_M = 1.0 \times 10^8$ ergs cm^{-2} s^{-1}, $P = 30$ s); in the second (case 3), the period is doubled ($F_M = 5.0 \times 10^7$ ergs cm^{-2} s^{-1}, $P = 60$ s). Because of the increased period in case 3, the waves of cases 1 and 3 suffer different amounts of radiation damping in the lower photosphere. Thus, although they have the same initial energy flux, the fraction remaining at the temperature minimum is larger for the wave with the longer period by a factor of about 2 (see Paper I, Fig. 5). Hence both cases 2 and 3 constitute wave calculations with doubled energy flux at the base of the chromosphere.

Figure 4 shows that the increase in the velocity amplitude by a factor of 1.4 increases the apparent temperature by a factor of about 3. The temperature enhancements for the waves of case 2 (case 3) reach 270 K (230 K) in the Mg II line and 170 K (150 K) in the Ca II line in the temperature minimum region ($z = 500$ km).

The *Skylab* observations used by Vernazza, Avrett, and Loeser (1981) for model F are made with a 5″ × 5″ resolution. In view of the sub-arcsec diameter of the magnetic flux tubes, an even larger disparity between a true flux-tube atmosphere and the average model C must be expected, implying that the wave amplitude may be still larger and the nonlinear behavior of the Planck function may result in an even higher temperature enhancement. We thus conclude that for plausible assumptions about the acoustic or slow-mode wave amplitudes the discrepancies between the empirical atmospheres can be accounted for.

e) Temperature Depression

An interesting and surprising feature of the above calculations is the depression of the time-averaged temperature distribution of the dynamical model relative to the initial radiative equilibrium model. This depression was found for all (solar) models of Paper I as well as for the stellar models (Schmitz and Ulmschneider 1981). As discussed in Paper I, this is a consequence of the nonlinear dependence of the source function in the energy equation on temperature. The magnitude of the temperature depression is uncertain, however, since it depends on simplifying assumptions about the (LTE or non–LTE) state of the gas, the temperature and pressure dependence of the opacity, and the number of wave trains that have propagated through the atmosphere before the temperature is determined (see below).

In order to elucidate the temperature depression, we consider a simplified energy equation. The equation satisfied by the time-averaged dynamical atmosphere is

$$\overline{\frac{dF_M}{dz}} = 4\pi\overline{\kappa\rho(J - B)}\,, \tag{8}$$

where κ is the gray absorption coefficient, J and B are the mean integrated intensity and the integrated Planck function, and F_M is the energy flux carried in the outward direction by the mechanical waves; the bar indicates time-averaging. Now, in the upper photosphere below the height of shock formation, the only process by which the waves lose a significant fraction of their energy is radiation damping, which becomes negligible at the low density in the layers near the temperature minimum (see Paper I, Fig. 5). In these layers, the waves travel nearly adiabatically. To a good approximation the left-hand side of equation (8) is zero, and thus the radiative terms alone must satisfy the energy equation, which is then very similar to the radiative equilibrium condition, except for the time-averaging.

The depression is most easily understood if one assumes the opacity to be constant. If one assumes further that the wave perturbs the temperature T about the steady state value $\bar{T}$ by the amount δT, i.e., $T = \bar{T} + \delta T$, the energy equation at the foot of the chromosphere may be written as

$$T_{RE}^4 = (\bar{T})^4[1 + 4\overline{(\delta T/\bar{T})} + 6\overline{(\delta T/\bar{T})^2} + \cdots]\,. \tag{9}$$

When the relative amplitude, $\delta T/\bar{T}$, becomes sufficiently large,

the nonlinear term forces the mean temperature, T, to be lower than the (initial) radiative equilibrium temperature, T_{RE} (see Fig. 1). The actual depression depends on the detailed temperature dependence of the opacity in the nongray non–LTE energy equation as well as on the wave profile and the number of waves that have passed the temperature minimum region.

The value of the temperature depression given in Paper I was too large because of a computational error in the frequency averaging of the opacity. A recalculation of the wave cases 1 and 2 with the Kurucz opacity table gave a much smaller temperature depression (see Fig. 4, dashed curves labeled *1* and *2*). It is interesting to note, however, that the temperature enhancement relative to the depressed mean temperature is not affected by the change in the opacity. The reason is that the enhancements are caused by the large wave amplitude and are very insensitive to the temperature of the ambient medium and to the choice of the opacity function, as can also be seen from Paper I, Figures 1, 2, and 5.

A more realistic treatment of the temperature depression would include the time-dependent effects of atomic and molecular line blanketing as well as departures from LTE. Such calculations have not been carried out and are quite difficult to perform. An obvious improvement of the present calculations would be to relax the assumption that the opacity is gray. However, test runs have shown that the effect is small (Schmitz, Ulmschneider, and Kalkofen 1984) because of the smooth frequency dependence of the H^- opacity, for which the Rosseland and Planck means do not differ greatly from one another or from the nongray opacity.

A further effect that tends to reduce the magnitude of the temperature depression without reducing the flux enhancement in the ultraviolet lines is due to the finite length of the expected wave trains. The computations reported here are based on piston motion at the base of the atmosphere that is initiated at some instant of time and continues until the medium has settled into a dynamically steady state, usually about 30 wave periods for the temperature minimum region, in which the mean values of temperature, density, and pressure no longer vary with time. For the assumed periods of the acoustic or slow-mode mhd waves this time span constitutes a perhaps unrealistically long coherence time of 15 min or more. If the waves are generated by the granulation elements in the convection zone, they ought to appear as wave packets with time spans at most as long as the average granulation lifetime of 8 min (Beckers 1981). If the lifetimes of the little bright dots (~ 3 min) seen in high-resolution pictures of the Sun near 1600 Å (Brueckner 1981, Fig. 3) are assumed to be more typical estimates for the lifetime of the wave packets, they may last for only six wave periods of 30 s. Similar conclusions may be drawn from the lifetime of 2–3 min of facular points in the solar filigree (Bruzek 1977, pp. 72–73). Thus the wave packets might exist for only about 20% of the time interval necessary to establish the dynamically steady state. Consequently the much less pronounced temperature depressions obtained for non-steady situations (see Paper I, Fig. 6) may be more appropriate. In the dynamical state the temperature depression continually increases with time as the atmosphere adjusts to the presence of the waves; but since the waves propagate nearly adiabatically in the temperature minimum region, the temperature enhancements in the Mg and Ca lines will not be affected. In Figure 4 we have indicated (*dotted curves*) the temperature depressions of cases 1 and 2 at the instant when eight waves have passed the temperature minimum region; the magnitude of the temperature depression is much reduced.

f) *The Silicon Continuum*

The minimum temperature in the transition region between photosphere and chromosphere of the VAL model is based not only on the infrared continuum near 0.15 mm but also on the Si continuum in the ultraviolet near 0.15 μm. The low temperature seen in the ultraviolet continuum may be surprising, since one might expect the same physical effect that produced the temperature enhancement in the ultraviolet lines to give an even larger enhancement in the Si continuum. The reason why this is not observed (in the dynamical model) is that the continuum radiation from the second level of Si in the range 0.152–0.168 μm is controlled by the photospheric radiation field (VAL), which arises in layers where the amplitude of the mechanical waves is very low. The influence of the local electron temperature on the Si populations is very weak, and the influence of large-amplitude waves on the emergent radiation in the Si continuum is therefore negligible.

IV. CONCLUSIONS

We have investigated the effect of mechanical waves in a time-dependent solar model on the emergent radiation field. These waves, which are acoustic waves in field-free regions and slow-mode mhd waves in regions of strong magnetic field, travel outward through the upper photosphere, where the density drop causes a corresponding increase in wave amplitude, which becomes large at the temperature minimum between photosphere and chromosphere. Because of the strong dependence on temperature of the Planck function for lines in the blue and ultraviolet regions of the spectrum, the excess of emission during the compressive phases of the waves exceeds the deficit of emission during the expansive phases; this results in an enhancement of the time-averaged flux in the lines, an effect that grows with decreasing optical wavelength.

When the observed fluxes in the K line of Ca II and the *k* line of Mg II are interpreted with the aid of time-independent models, a temperature enhancement is inferred that is larger for the *k* line of Mg than for the K line of Ca. The lowest value of the temperature is measured in the infrared continuum, which may be depressed below that of the undisturbed atmosphere. The layer where the maximal effect on empirical temperatures is expected is the temperature minimum region.

Qualitatively, the predicted systematic dependence of the minimum temperatures on the wavelength of the diagnostic feature agrees with the temperatures of the empirical models. Quantitatively, the temperature enhancements from the energy fluxes expected for acoustic waves in field-free regions are too small to explain fully the differences between the empirical solar models. But for plausible energy fluxes in slow-mode mhd waves expected in magnetic flux tubes the temperature enhancements are large enough to account fully for the differences between the models.

The explanation for the different temperatures in solar models has implications also for empirical models of late-type stars, where the structure of the transition region between photosphere and chromosphere is based on the observed Ca II and Mg II line fluxes. The conclusion drawn from the present work is that the minimum temperatures in these stellar models are higher than the observed mean temperatures and lower than the temperatures inferred from the resonance lines of ionized calcium and magnesium. This may have further implications for the inferred mass of stellar chromospheres and for the energy required to support them.

The authors thank E. H. Avrett, J. W. Leibacher, and R. Wehrse for critical comments on the manuscript. W. K. is grateful to the Alexander von Humboldt Foundation for a Senior U.S. Scientist award. This work has been supported in part by NASA grant NAGW-253, NSF grant AST 83-03522, and the Deutsche Forschungsgemeinschaft (SFB 132).

REFERENCES

Avrett, E. H. 1977, in *The Solar Output and Its Variation*, ed. O. R. White (Boulder: Colorado Associated University Press), p. 327.
———. 1981, in *Solar Phenomena in Stars and Stellar Systems*, ed. R. M. Bonnet and A. K. Dupree (Dordrecht: Reidel), p. 173.
Ayres, T. R. 1975, *Ap. J.*, **201**, 799.
———. 1981, *Ap. J.*, **244**, 1064.
Ayres, T. R., and Linsky, J. L. 1976, *Ap. J.*, **205**, 874.
Basri, G. S., and Linsky, J. L. 1979, *Ap. J.*, **234**, 1023.
Beckers, J. M. 1981, in *The Sun as a Star*, ed. S. Jordan (NASA SP-450; Washington, D.C.: GPO), p. 24.
Brueckner, G. E. 1981, *Space Sci. Rev.*, **29**, 407.
Bruzek, A. 1977, in *Illustrated Glossary for Solar and Solar-Terrestrial Physics*, ed. A. Bruzek and C. J. Durrant (Dordrecht: Reidel), p. 72.
Gingerich, O., Noyes, R. W., Kalkofen, W., and Cuny, Y. 1971, *Solar Phys.*, **18**, 347 (HSRA).
Gouttebroze, P., and Leibacher, J. W. 1980, *Ap. J.*, **238**, 1134.
Grant, I. P., and Peraiah, A. 1972, *M.N.R.A.S.*, **160**, 239.
Hui, A. K., Armstrong, B. H., and Wray, A. A. 1978, *J. Quant. Spectrosc. Rad. Transf.*, **19**, 509.
Kalkofen, W. 1981, in *Second Cambridge Workshop on Cool Stars, Stellar Systems, and the Sun* (SAO Special Rept. 392), p. 59.
Kelch, W. L. 1978, *Ap. J.*, **222**, 931.
Kelch, W. L., Linsky, J. L., Basri, G. S., Chiu, H. Y., Chang, S. H., Maran, S. P., and Furenlid, I. 1978, *Ap. J.*, **220**, 962.
Kelch, W. L., Linsky, J. L., and Worden, S. P. 1979, *Ap. J.*, **229**, 700.
Kurucz, R. 1979, *Ap. J. Suppl.*, **40**, 1.
Linsky, J. L. 1980, *Ann. Rev. Astr. Ap.*, **18**, 439.
Linsky, J. L., and Ayres, T. R. 1978, *Ap. J.*, **220**, 619.
Mihalas, D. 1978, *Stellar Atmospheres* (San Francisco: Freeman).
Peraiah, A. 1978, *Kodaikanal Obs. Bull.*, *A*, **2**, 115.
Peraiah, A., and Grant, I. P. 1973, *J. Inst. Math. Applics*, **12**, 75.
Schmitz, F., and Ulmschneider, P. 1981, *Astr. Ap.*, **93**, 178.
Schmitz, F., Ulmschneider, P., and Kalkofen, W. 1984, in preparation.
Shine, R. A. 1973, Ph.D. thesis, University of Colorado.
Shine, R. A., Milkey, R. W., and Mihalas, D. 1975, *Ap. J.*, **199**, 724.
Ulmschneider, P. 1979, *Space Sci. Rev.*, **24**, 71.
Ulmschneider, P., and Kalkofen, W. 1977, *Astr. Ap.*, **57**, 199.
Ulmschneider, P., Schmitz, F., Kalkofen, W., and Bohn, H. U. 1978, *Astr. Ap.*, **70**, 487 (Paper I).
Ulmschneider, P., and Stein, R. F. 1982, *Astr. Ap.*, **106**, 9.
Vernazza, J. E., Avrett, E. H., and Loeser, R. 1973, *Ap. J.*, **184**, 605.
———. 1976, *Ap. J. Suppl.*, **30**, 1 (VAL).
———. 1981, *Ap. J. Suppl.*, **45**, 635.
Wiese, W. L., Smith, M. W., and Miles, B. M. 1969, *Atomic Transition Probabilities*, Vol. **2** (NSRDS-NBS 22; Washington: GPO).
Withbroe, G. L., and Noyes, R. W. 1977, *Ann. Rev. Astr. Ap.*, **15**, 363.

W. KALKOFEN: Harvard-Smithsonian Center for Astrophysics, 60 Garden Street, Cambridge, MA 02138

P. ULMSCHNEIDER and F. SCHMITZ: Institut für Theoretische Astrophysik, Im Neuenheimer Feld, 6900 Heidelberg, Federal Republic of Germany